

## Eastern North Pacific Hurricane Season of 2007

LIXION A. AVILA AND JAMIE RHOME

*National Hurricane Center, NOAA/NWS/NCEP, Miami, Florida*

(Manuscript received 16 December 2008, in final form 10 February 2009)

### ABSTRACT

The hurricane season of 2007 in the eastern North Pacific Ocean basin is summarized, individual tropical cyclones are described, and a forecast verification is presented. The 2007 eastern North Pacific season was not an active one. There were 11 tropical storms, of which only 4 became hurricanes. Only one cyclone became a major hurricane. One hurricane struck Mexico and one tropical storm made landfall near the Guatemala–Mexico border. The 2007 National Hurricane Center forecast track errors were lower than the previous 5-yr means at all forecast lead times, and especially so for the 72-, 96-, and 120-h periods when the errors were 16%, 22%, and 20% lower, respectively. The official intensity forecasts had only limited skill.

### 1. Overview

After a year of above-normal activity in 2006 (Pasch et al. 2009) tropical cyclone activity in the eastern North Pacific Ocean basin returned to the relative low levels that have prevailed in most of the years since 1995. Eleven tropical storms developed and only four of these strengthened into hurricanes. Furthermore, only one cyclone intensified into a major hurricane [category 3 or higher on the Saffir–Simpson Hurricane Scale (Saffir 1973; Simpson 1974)]. These totals are well below the 1971–2006 average of 15 tropical storms, 9 hurricanes, and 4 major hurricanes. Four additional tropical depressions formed during the 2007 season but failed to strengthen into tropical storms. Category 1 Hurricane Henriette was the only Pacific basin hurricane to hit Mexico, causing nine deaths. Barbara made landfall as a tropical storm near the Mexico–Guatemala border.

A useful measure of overall season activity is the accumulated cyclone energy (ACE) index, which reflects the combined intensity and duration of the entire season's storms. This index is calculated by summing the squares of the wind speeds (in knots) for all tropical cyclones while at or above tropical storm strength. The ACE for 2007 in the eastern North Pacific was  $34 \times 10^4$  kt<sup>2</sup> or about 31% of the long-term (1971–2006) mean value of 113. This is the second lowest value since reli-

able records began in 1971. Only 1977 was less active by this measure.

The 2007 season began close to the average start date of the first tropical storm, with the formation of Tropical Storm Alvin on 27 May, immediately followed by the formation of Tropical Storm Barbara on 29 May. The long-term (1971–2006) median start day is 29 May. No other named cyclone developed until the depression that eventually became Hurricane Cosme formed on 14 July. Flossie was the only major hurricane of the season and the intensification occurred just before it entered the central Pacific hurricane basin at 140°W.

Using analysis techniques described by Avila et al. (2003), most of the tropical cyclones formed from tropical waves that can be traced westward from the Atlantic basin into the eastern North Pacific. Figure 1 shows the shower activity associated with several tropical waves moving from the Caribbean Sea westward across Central America and into the eastern North Pacific. In particular, one can see the westward propagation of the convection associated with the wave that crossed Central America on 28 August. This wave was marked by a well-defined northeast–southeast cyclonic wind shift extending from the surface to near 300 mb (hPa) and by the upward extension of moisture to near 200 mb trailing the wave axis, as shown in Fig. 2. This wave eventually triggered the development of Hurricane Henriette.

Vertical wind shear is a factor in controlling tropical cyclone genesis and intensification. Figure 3 shows the 200–850-mb vertical wind shear anomaly for July–October 2007. The figure reveals that stronger than normal

---

*Corresponding author address:* Dr. Lixion A. Avila, National Hurricane Center, 11691 SW 17th St., Miami, FL 33165.  
E-mail: lixion.a.avila@noaa.gov

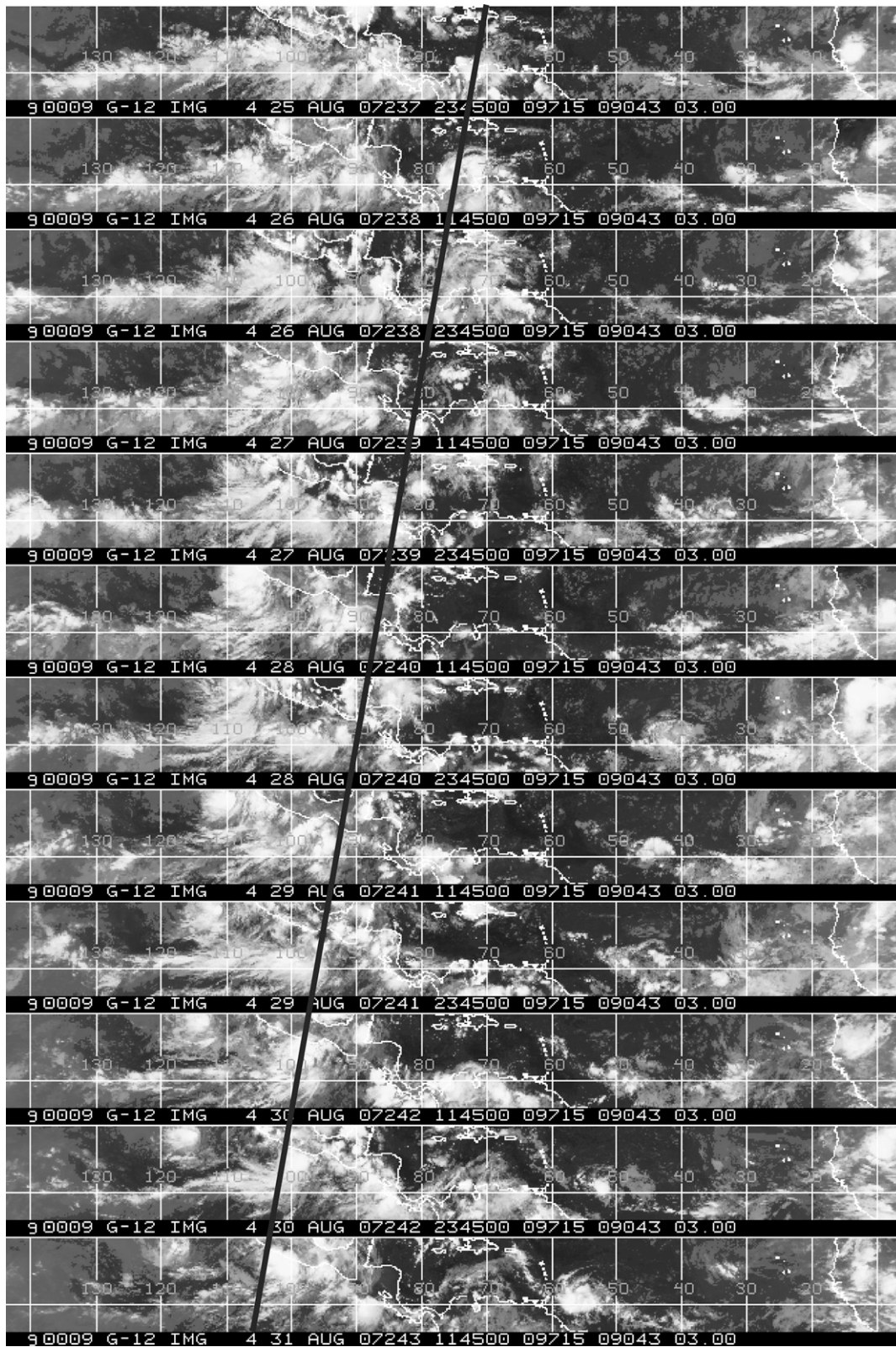


FIG. 1. Time sequence of GOES infrared images taken twice per day at 1145 and 2345 UTC from 25 to 31 Aug 2007. The latitude belt is roughly 5°–20°N.

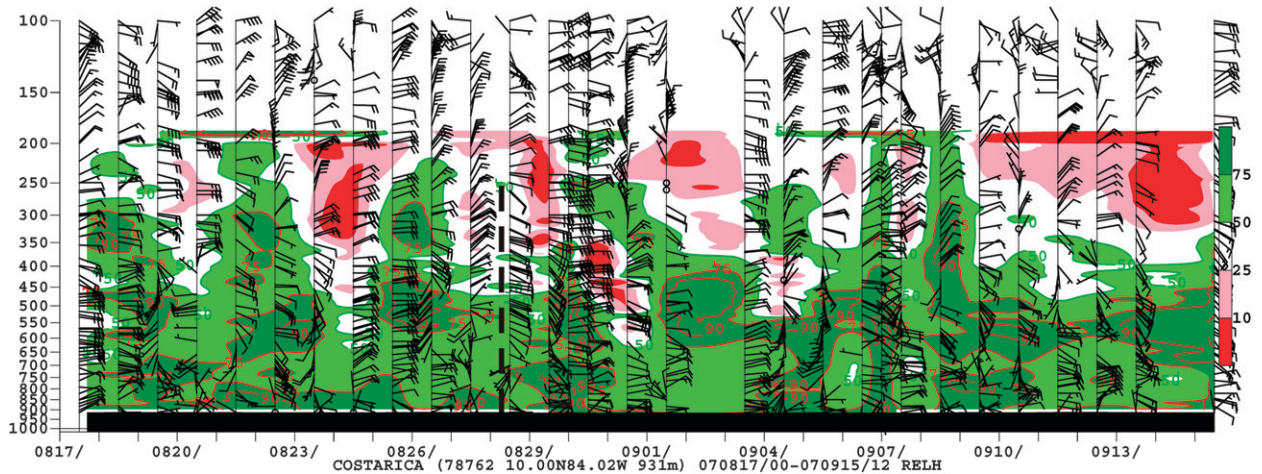


FIG. 2. Vertical time section of wind and relative humidity at Costa Rica from 17 Aug to 14 Sep 2007. Winds and moisture are plotted every 12 h (when available) according to convention with each full and half barb denoting 5 and 10 kt, respectively. Dashed line marks the axis of the tropical wave as it passed the station.

easterly shear prevailed through most of the season south of  $16^{\circ}\text{N}$  and between  $100^{\circ}$  and  $125^{\circ}\text{W}$ . Historically, most of the eastern North Pacific tropical cyclone genesis occurs within this region. Because the shear was high, the shower activity associated with most of the incipient tropical cyclones was continuously separated from the area of minimum pressure. Consequently, the cyclones did not strengthen until they moved into areas where the shear was lighter as noted in Fig. 3. By then, many of the incipient cyclones were already close to cooler waters and moving into a more stable environment. This resulted in a relatively high number of weak short-lived cyclones during the season, and contributed to the unusually low seasonal ACE index noted above.

A summary of the life cycle of each of the 2007 season's named tropical cyclones is provided in section 2.

Section 3 provides verification statistics on official National Hurricane Center (NHC) forecasts of these cyclones.

## 2. Tropical cyclone summaries

Summaries of individual cyclones in this section are based on NHC's poststorm meteorological analyses. These analyses result in the creation of a "best track" database for each storm, consisting of 6-hourly representative estimates of the cyclone's center location, maximum sustained (1-min average) surface (10 m) wind, and minimum sea level pressure. The life cycle of each cyclone (corresponding to the dates given in Table 1 for the season's tropical storms and hurricanes) includes the tropical depression stage, but it does not include the

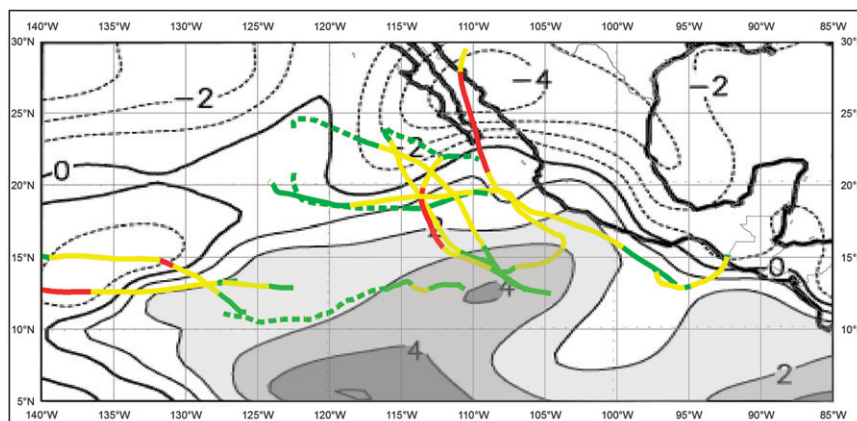


FIG. 3. Anomaly from the long-term mean of wind shear ( $\text{m s}^{-1}$ ) for July–October 2007 with the 2007 tracks of all named tropical cyclones. Areas of stronger-than-normal wind shear are shaded. Data were provided by the NOAA/Climate Prediction Center.

TABLE 1. Eastern North Pacific tropical storms and hurricanes of 2007.

Storm	Class*	Dates**	Max 1-min wind (kt)	Min sea level pressure (mb)	Direct deaths
Alvin	T	27–31 May	35	1003	
Barbara	T	29 May–2 Jun	45	1000	
Cosme	H	14–22 Jul	65	987	
Dalila	T	22–27 Jul	50	995	
Erick	T	31 Jul–2 Aug	35	1004	
Flossie	H	8–16 Aug	120	949	
Gil	T	29 Aug–2 Sep	40	1001	
Henriette	H	30 Aug–6 Sep	75	972	9
Ivo	H	18–23 Sep	70	980	
Juliette	T	29 Sep–2 Oct	50	997	
Kiko	T	15–23 Oct	60	991	

\* Tropical storm (T), wind speed 34–63 kt ( $17\text{--}32\text{ m s}^{-1}$ ); hurricane (H), wind speed 64 kt ( $33\text{ m s}^{-1}$ ) or higher.

\*\* Dates begin at 0000 UTC and include the tropical depression stage but exclude the remnant low stage.

remnant low stage. The tracks for the season’s tropical storms and hurricanes, including their tropical depression and remnant low stages (if applicable), are shown in Fig. 4.

Observations in eastern North Pacific tropical cyclones are generally limited to satellite data, primarily from the Geostationary Operational Environmental Sat-

ellites (GOES). GOES-East and GOES-West provide the visible and infrared imagery that serves as input for intensity estimates using the Dvorak (1984) classification technique. This imagery is supplemented by occasional microwave satellite data and imagery from National Oceanic and Atmospheric Administration (NOAA) polar-orbiting satellites, Defense Meteorological Satellite Program (DMSP) satellites, the National Aeronautics and Space Administration (NASA) Tropical Rainfall Measuring Mission (TRMM), and the NASA Quick Scatterometer (QuikSCAT) and the Department of Defense WindSat among others. While passive microwave imagery is useful for tracking tropical cyclones and assessing their structure, both QuikSCAT and WindSat retrieve estimates of ocean surface vector winds across a fairly wide swath, and with careful interpretation can provide occasional estimates of the location, intensity, and outer wind radii of a tropical cyclone. There was only one aircraft reconnaissance mission conducted by the 53rd Weather Reconnaissance Squadron of the U.S. Air Force Reserve Command (AFRC) into eastern North Pacific tropical cyclones during 2007; that mission was in Hurricane Henriette. Land-based radars from the Meteorological Service of Mexico and observations from both the Meteorological Service of Mexico and the Mexican Navy were extremely useful for monitoring tropical cyclones during 2007.

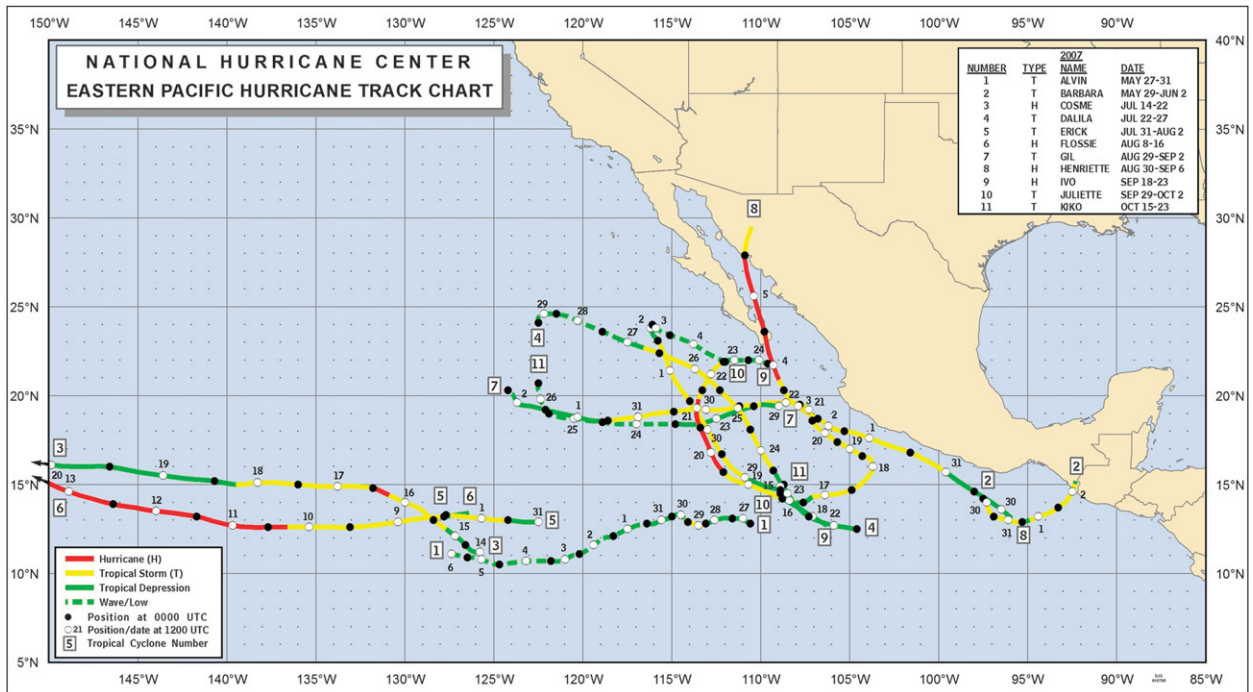


FIG. 4. Track chart of eastern North Pacific tropical storms and hurricanes of 2007.

*a. Tropical Storm Alvin, 27–31 May*

Alvin developed from a poorly defined tropical wave that crossed Dakar, Senegal, on 9 May. The wave moved westward across the Atlantic Ocean and the Caribbean Sea with very little associated thunderstorm activity until the wave reached Central America on 20 May. The wave continued westward across the eastern North Pacific with a gradual increase in the associated shower activity, and developed an exposed surface circulation center. The convection became a little better organized and it is estimated that a tropical depression formed at 0000 UTC 27 May about 300 n mi south of the southern tip of Baja California.

There was little change in the depression's organization during the next day or so while it moved slowly westward, with its center continuing to be displaced from the convection. A small relaxation of the easterly shear resulted in slight strengthening, and the cyclone became a tropical storm at 0000 UTC 29 May with a peak intensity of 35 kt and a minimum pressure of 1003 mb. Thereafter, Alvin weakened as it moved westward into an environment of stable air and higher shear. It is estimated that the cyclone became a remnant low at 0000 UTC 1 June. During the next few days, Alvin's remnants were steered by the low-level flow on a general west-southwestward and westward track. The remnant low dissipated at 1800 UTC 6 June.

*b. Tropical Storm Barbara, 29 May–2 June*

The genesis of Barbara appears to have been associated with a tropical wave that left the west coast of Africa on 14 May. The wave crossed Central America on 25 May and emerged over the eastern North Pacific the next day. The wave interacted with the intertropical convergence zone, and on 27 May a broad area of surface low pressure formed a couple hundred miles south of Puerto Escondido, Mexico. Limited and disorganized shower activity accompanied the low as it edged northward during the next couple of days. On 29 May, however, convection increased and became more concentrated near the center of the low, and a tropical depression formed by 1800 UTC that day about 100 n mi south-southeast of Puerto Escondido.

Initially stationary, the depression did not gain any strength during the first 12 h or so following genesis. The cyclone then intensified gradually on 30 May while inching toward the south-southeast within an environment of very weak steering currents. It became a tropical storm by 1200 UTC that day and 6 h later it reached an intensity of 40 kt. Northerly wind shear contributed to Barbara's weakening early on 31 May, and the storm moved very slowly eastward that day under the influence

of a mid- to upper-level trough over the western Gulf of Mexico. By 0000 UTC 1 June, the cyclone had weakened to a tropical depression while centered about 200 n mi west-southwest of the Mexico–Guatemala border. Later that day, however, as wind shear decreased, Barbara strengthened over warm waters and reached an intensity of 45 kt by 1200 UTC 1 June. By that time the storm had also begun a general northeastward motion at about 6 kt that would continue during the next 24 h. The intensity also remained steady during that period, and Barbara made landfall at about 1300 UTC 2 June, roughly 20 n mi northwest of the Mexico–Guatemala border, with maximum sustained winds of 45 kt. The cyclone quickly deteriorated inland over the rugged terrain of extreme southeastern Mexico while passing near the town of Tapachula. Barbara became a depression by 1800 UTC 2 June and completely dissipated by the end of that day.

No ship reports of sustained winds of tropical storm force were reported in association with Barbara. Sustained winds of 40 kt were reported, however, at Tecun Uman, Guatemala (located near the border with Mexico about 15 miles from the Pacific coast), near the time of Barbara's landfall on the morning of 2 June. An automated surface station at Puerto Madero, Mexico, operated by the Mexican Navy, reported sustained winds of 31 kt with gusts to 46 kt near the time of landfall. Nearly 5 in. of rain was reported on 2 June at Huixtla, Mexico. A few other reports of 2–4 in. of rain in extreme southeastern Mexico were also received.

Barbara's winds damaged roofs and downed trees in Mexico and Guatemala in coastal areas near the border between the two countries. Rain-induced river floods led to a bridge being washed out in coastal Guatemala. There were reports of significant damage to agricultural crops in southeastern Mexico, with an estimated cost of more than \$50 million (U.S. dollars).

*c. Hurricane Cosme, 14–22 July*

Cosme originated from a tropical wave that emerged off the coast of Africa on 27 June. The wave was difficult to track across the Atlantic Ocean and Caribbean Sea because of a lack of convective activity, but is estimated to have entered the eastern North Pacific basin around 8 July. The wave began to show signs of organization on 10 July, but remained embedded within the intertropical convergence zone for the next couple of days and was slow to develop a well-defined circulation. After separating from the ITCZ on 13 July, the system gradually gained convective organization and became a tropical depression by 1200 UTC 14 July, while centered about 1725 n mi east-southeast of Hilo, Hawaii.

The depression had a very large circulation and initially moved slowly toward the northwest in response to

a weakness in a high pressure ridge to the north. Once convection deepened and a well-defined banding feature developed on 15 July, the cyclone became a tropical storm at 1800 UTC that same day. While over warm waters and within an environment of low vertical wind shear, Cosme reached hurricane strength on 16 July while centered about 1400 n mi east of Hilo. The strengthening episode was short lived, however, and Cosme only maintained hurricane status for 6 h.

Cosme then moved toward the west as the ridge to the north strengthened. By early on 17 July, the cyclone reached an environment of moderate easterly shear and 25°C waters, and weakened to a tropical storm. Cosme slowly weakened as it moved westward, and became a tropical depression at 1800 UTC 18 July, about 900 n mi east-southeast of Hilo. The depression continued westward and crossed 140°W into the central North Pacific basin around 0000 UTC 19 July. The depression continued westward for the next 4 days and remained well to the south of the Hawaiian Islands. The cyclone degenerated to a remnant low late on 22 July, about 180 n mi east-southeast of Johnston Island, and dissipated by 1800 UTC 24 July, about 570 n mi west of Johnston Island.

#### *d. Tropical Storm Dalila, 22–27 July*

Dalila formed from a tropical wave that entered the eastern North Pacific Ocean on 17 July. The wave spawned a broad area of low pressure several hundred nautical miles south-southeast of the Gulf of Tehuantepec on 19 July. As the low moved west-northwestward during the next couple of days, the associated shower activity gradually increased. Additional development during the next 24 h led to the formation of a tropical depression at 0000 UTC 22 July about 400 n mi south of Manzanillo, Mexico.

Northeasterly shear inhibited significant strengthening and the cyclone remained a tropical depression for the next 2 days. The depression moved west-northwestward during the first 24 h of its existence, but then turned northwestward on 23 July around the southwestern portion of a midlevel ridge centered over northern Mexico. The shear decreased late on 23 July and allowed thunderstorm activity to form closer to the circulation center. The depression strengthened and became a tropical storm at 0000 UTC 24 July, while located about 350 n mi southwest of Manzanillo. Thereafter, the shear continued to relax and Dalila gradually intensified, reaching a peak intensity of 50 kt at 0000 UTC 25 July. Dalila continued moving northwestward and its center passed over or very near Socorro Island just after 0600 UTC 25 July. The next day the tropical storm turned west-northwestward, and began moving over progressively cooler water that initiated a weakening trend.

Dalila weakened to a tropical depression at 0600 UTC 27 July and degenerated to a remnant low 12 h later, while located about 400 n mi west of the southern tip of Baja California. The remnant low moved west-northwestward during the next couple days before slowing down and turning west-southwestward on 29 July. It then drifted southward on 30 July and dissipated about 700 miles west of the southern tip of Baja California around 1200 UTC that day.

Four QuikSCAT passes between 1313 UTC 23 July and 0115 UTC 25 July were helpful in determining the intensity of Dalila during this time. The estimated peak intensity of 50 kt was based on data from the 0115 UTC 25 July QuikSCAT pass. Because Dalila was an unusually large tropical cyclone, the corresponding estimated minimum pressure is a little lower than what the standard Dvorak pressure–wind relationship yields.

#### *e. Tropical Storm Erick, 31 July–2 August*

The tropical wave that eventually led to the formation of Erick departed western Africa on 16 July. The wave passed through the Lesser Antilles on 22 July with some deep convection, but thunderstorm activity remained disorganized for the next several days. The system moved across Central America on 25 July, and a weak low pressure area formed along the wave axis in the eastern Pacific on 28 July. Easterly wind shear prevented development of the low for a few days as associated deep convection remained well west of the low. Early on 31 July, however, thunderstorms formed closer to the center of the low, and it is estimated that the system gained enough organization to be classified as a tropical depression at 1200 UTC that day, located about 925 n mi southwest of the southern tip of Baja California.

Despite easterly shear, the depression intensified into a tropical storm early on 1 August, but reached a peak intensity of only 35 kt. The easterly shear never relented, and Erick weakened to a tropical depression at 0000 UTC 2 August, while located about 1175 n mi west-southwest of the southern tip of Baja California. The surface low lost its well-defined circulation as it became elongated from northeast to southwest. The depression degenerated into a tropical wave by 0600 UTC 2 August, and its remnants continued moving westward. A weak low reformed within the wave on 3 August before entering the central North Pacific basin early on 4 August. The low dissipated several hundred miles southwest of the Hawaiian Islands on 8 August.

#### *f. Hurricane Flossie, 8–16 August*

Flossie's genesis was probably triggered by an ill-defined tropical wave that moved from Africa into the eastern tropical Atlantic on 21 July. This wave moved

across the Atlantic basin with little associated deep convection, and crossed Central America on 1 August. An area of showers and thunderstorms then developed near the Gulf of Tehuantepec on 2 August. The disturbed weather area moved generally westward with little change in organization during the next couple of days. There was some increase in the organization of the deep convection on 4 August, while the disturbance was centered roughly 800 n mi south of the southern tip of Baja California, Mexico. Little further change in the system occurred until 6 August, when it acquired nearly enough organization to be considered a tropical depression. However, deep convection failed to persist near the low-level circulation center. The disturbance continued to move generally westward and, by 1800 UTC 8 August, the system exhibited sufficiently organized and persistent deep convection to designate the formation of a tropical depression. It was then centered about 1700 n mi east-southeast of the Hawaiian Islands.

Within an environment of diffluent upper-level anticyclonic flow, low vertical shear, and warm ocean waters, the tropical cyclone strengthened and became a tropical storm by 0000 UTC 9 August. For the next several days, environmental conditions remained conducive for intensification, and Flossie strengthened into a hurricane by 1200 UTC 10 August, when an eye became evident in both infrared and visible satellite imagery. A subtropical ridge persisted to the north of the cyclone, which forced a continued westward motion. Flossie continued to intensify and by 1200 UTC 11 August, just before it entered the central Pacific hurricane basin, the system became a category 4 hurricane on the Saffir-Simpson Hurricane Scale based on objective Dvorak T numbers. Flossie reached its estimated peak intensity of 120 kt early on 12 August, while centered about 850 n mi east-southeast of Hawaii. The hurricane moved west-northwestward over the next couple of days while maintaining category 4 strength. By early on 14 August, increasing vertical shear caused weakening. As Flossie neared Hawaii, it turned westward while continuing to lose strength. Flossie's center passed about 90 n mi south of South Point on the Island of Hawaii early on 15 August causing minimal impacts. Continuing westward and well to the south of the remaining Hawaiian Islands, the cyclone steadily weakened in an environment of strong upper-level southwesterly winds. Flossie weakened to a tropical storm by 1200 UTC 15 August and to a depression by early on 16 August. The system then quickly degenerated into a remnant low and dissipated.

*g. Tropical Storm Gil, 29 August–2 September*

A vigorous tropical wave left the west coast of Africa, on 16 August. The wave had a large amplitude, abun-

dant convection, and 24-h pressure falls on the order of 6 mb. The wave moved westward over the tropical Atlantic for several days maintaining its large cyclonic envelope and intermittent thunderstorm activity. The wave became less distinct on the 21 August when it interacted with a large upper-level trough centered over the eastern Caribbean Sea. The wave continued westward across the Caribbean Sea and Central America, and the northern portion of the wave spawned a weak low pressure area in the Bay of Campeche on 26 August. However, most of the convective activity associated with the southern portion of the wave continued westward over Mexico.

The wave emerged over the eastern North Pacific on 27 August, and the shower activity became concentrated just south of Cabo Corrientes. The system continued westward and became better organized as it developed additional thunderstorms with a few convective bands. It is estimated that a tropical depression formed at 1200 UTC 29 August about 240 n mi south-southeast of the southern tip of Baja California, and it became a tropical storm 6 h later. The center of Gil was located on the northeastern edge of the convection due to strong northeasterly shear, which inhibited further intensification. The cyclone's peak winds reached only 40 kt and a minimum pressure of 1001 mb occurred at 1200 UTC 30 August. Thereafter, gradual weakening occurred due to both shear and cooler waters. Gil became a westward-moving remnant low at 1800 UTC 2 September and dissipated later that day.

*h. Hurricane Henriette, 30 August–6 September*

Henriette originated from a tropical wave that departed the west coast of Africa on 20 August and moved uneventfully across the tropical Atlantic. The wave produced some convection in the Caribbean Sea but reached Central America on 28 August before any significant development could occur. By 29 August the wave had moved westward into the eastern North Pacific basin, producing disorganized showers and thunderstorms, and late that day a small area of low pressure developed in association with the wave about 350 n mi southeast of Acapulco, Mexico. Convection associated with the low improved in organization early on 30 August, and by 0600 UTC that day the system became a tropical depression about 315 n mi southeast of Acapulco.

The cyclone initially headed toward the west-northwest around a subtropical ridge that was centered over the western Gulf of Mexico. It gained organization and became a tropical storm by 1200 UTC 31 August, centered about 75 n mi south of Acapulco. During the next 36 h, Henriette slowly strengthened and continued west-northwestward parallel to the Pacific coast of Mexico,

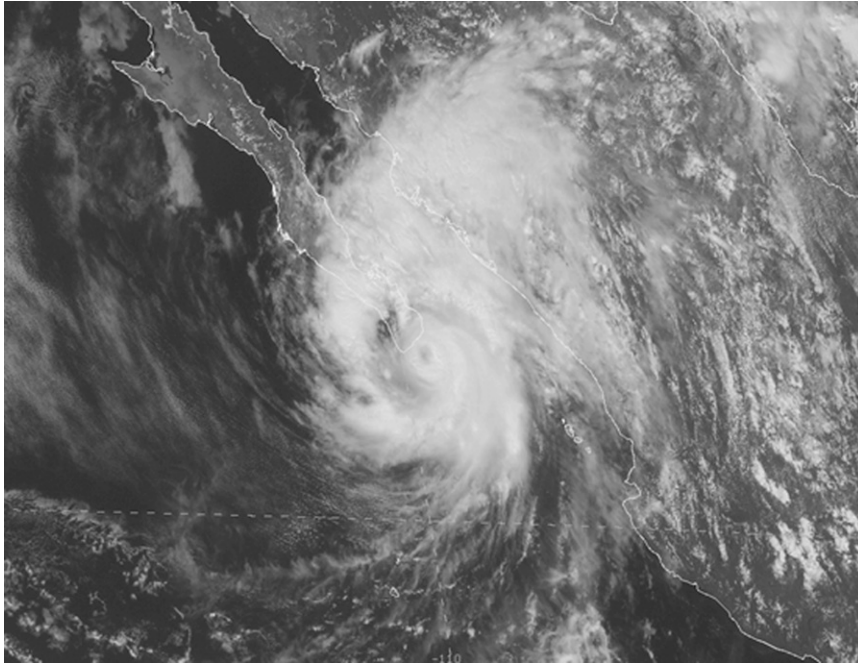


FIG. 5. *GOES-11* visible image of Hurricane Henriette at 1900 UTC 4 Sep 2007, just prior to landfall.

with its center passing roughly 40–50 n mi offshore. Despite not making landfall during this period, the storm brought heavy rainfall to portions of the coast, especially near Acapulco.

Henriette turned westward and away from the Pacific coast of Mexico late on 1 September as the subtropical ridge built westward over northern Mexico. By 0600 UTC the next day, Henriette had reached an intensity of 55 kt while centered about 95 n mi southwest of Manzanillo. The storm remained just shy of hurricane strength for the next 2 days as it headed generally northwestward, passing about 175 n mi west of Cabo Corrientes. At about 0600 UTC 4 September, Henriette reached hurricane status as it turned north-northwestward toward the Baja California peninsula, ahead of a midlatitude trough approaching the west coast of the United States. The hurricane reached its peak intensity of 75 kt at 1200 UTC that day while centered about 75 n mi south-southeast of the southern tip of Baja California. Henriette then made landfall near San Jose del Cabo on the southern tip of Baja California, at about 2100 UTC 4 September with maximum winds near 70 kt. Figure 5 depicts Hurricane Henriette just prior to making landfall in Baja California. Continuing north-northwestward, Henriette emerged over the Gulf of California early on 5 September. The interaction with land caused a slight weakening, but Henriette remained a category 1 hurricane for most of that day. Very late on 5 September,

however, Henriette began to weaken. It made its final landfall along the Gulf of California coast of mainland Mexico, near Guaymas, at about 0000 UTC 6 September with an estimated intensity of 60 kt. Henriette deteriorated quickly over land and dissipated over the mountains of northwestern Mexico shortly after 0600 UTC that day.

The Air Force reconnaissance aircraft made two center “fixes” during a single reconnaissance mission into Henriette on 3 September. The central pressure on the last fix was 981 mb, a central pressure typically associated with hurricane intensity, but maximum flight-level winds at 850 mb during the mission were only 71 kt, and the maximum surface wind speed estimate from the SFMR was 58 kt. These data support the best-track intensity of 60 kt at 1800 UTC 3 September. Geostationary satellite imagery suggests that Henriette slowly gained organization during the following several hours and became a hurricane early the next day. The peak intensity of 75 kt at 1200 UTC 4 September is based on subjective Dvorak intensity estimates.

No ship reported winds of tropical storm force in association with Henriette. A sustained wind of 66 kt and a gust to 102 kt were reported at Ciudad Obregon in the Mexican state of Sonora, at 2100 UTC 5 September (about 3 h prior to the final landfall of Henriette). This station is situated several miles inland at an elevation of about 50 m above sea level, and was about 50 n mi east of the center of Henriette at the time of this observation.

The 66-kt observation appears likely to be an overestimate of a sustained wind at 10 m. Rainfall totals of 125–225 mm were common in the states of Oaxaca and Guerrero while the center of Henriette passed just offshore during 30 August–1 September. Similar amounts fell over the southern Baja California peninsula and in the state of Sonora during 4–6 September.

Media reports indicate at least nine fatalities in Mexico are directly attributable to Henriette. Six of these deaths occurred near Acapulco as a result of mud slides induced by heavy rains while the center of Henriette passed just offshore. Two fishermen perished near the coast of Sonora in the region where Henriette made its final landfall, and one person died in the surf along the southern Baja California Peninsula. Media reports indicate that Henriette caused about \$25 million in damage in the Mexican state of Sonora.

*i. Hurricane Ivo, 18–23 September*

Ivo developed from a tropical wave that moved across the west coast of Africa on 1 September. There was little convection associated with the wave during its passage across the Atlantic basin until it reached the western Caribbean Sea. The wave crossed Central America and entered the eastern North Pacific basin on 15 September, when the wave began to show signs of increased organization. A broad area of low pressure formed within the wave the next day and the organization of the system gradually increased as the low moved westward. A tropical depression formed around 0600 UTC 18 September, about 400 n mi south-southwest of Manzanillo.

The depression initially moved west-northwestward to the south of a midlevel ridge that extended westward from northern Mexico. Under light northwesterly shear, the cyclone strengthened, becoming a tropical storm by 0000 UTC 19 September, about 525 n mi south of the southern tip of Baja California. Ivo continued to strengthen and became a hurricane at 0000 UTC 20 September, about 450 n mi south-southwest of the southern tip of Baja California. As a large deep-layer low moved southward into California, the western periphery of the subtropical ridge eroded, and Ivo turned northwestward on 20 September. During the day microwave imagery showed a well-defined eye, although the eye was only intermittently visible in conventional satellite imagery; Ivo reached its estimated peak intensity of 70 kt around 1800 UTC that day. This estimated maximum intensity of 70 kt was based on a blend of subjective Dvorak estimates of 77 kt and objective (ADT) estimates of around 65 kt from the University of Wisconsin/Cooperative Institute for Meteorological Satellite Studies.

Early on 21 September, westerly flow associated with the large upper low began to undercut the outflow of

Ivo, and the cyclone began to weaken. As Ivo turned northward around the periphery of the subtropical ridge, the cloud pattern began to deteriorate, and Ivo weakened to a tropical storm around 1800 UTC that day about 275 n mi southwest of the southern tip of Baja California. Ivo turned to the north-northeast on 22 September, and even though it remained over warm waters, the cyclone continued to weaken within increasing westerly shear as it approached Baja California. The cyclone weakened to a depression near 0000 UTC 23 September about 130 n mi west-southwest of the southern tip of Baja California. Deep convection associated with the cyclone diminished, and Ivo degenerated into a remnant low later that day about 80 n mi southwest of the southern tip of Baja California. The remnant low moved slowly eastward and dissipated early on 25 September.

*j. Tropical Storm Juliette, 29 September–2 October*

Juliette formed from a tropical wave that moved off the coast of west Africa early on 12 September. The wave became indistinct over the central Atlantic Ocean during 17–19 September as it interacted with another slower-moving tropical wave located to its west, but ultimately became better defined on 20 September over the eastern Caribbean. It then enhanced a preexisting area of showers and thunderstorms located over the western Caribbean Sea on 22 September and moved inland over Central America soon thereafter. The southern portion of the wave emerged over the eastern Pacific Ocean on 23 September and continued to move westward over the next few days with showers and thunderstorms becoming more consolidated on 26 September. An area of low pressure developed along the wave axis around 1200 UTC 27 September, approximately 300 n mi southwest of Acapulco. Deep convection gradually became better organized near the low during the next day or so, and a tropical depression is estimated to have formed at 0000 UTC 29 September, centered about 365 n mi southwest of Manzanillo.

The depression intensified to a tropical storm about 12 h later, and moved to the northwest over the next 3 days at a fairly consistent speed of about 10 kt around the western periphery of a midlevel ridge located over northern Mexico. Juliette gradually strengthened and reached a peak intensity of 50 kt at 1200 UTC 30 September as it passed between Socorro and Clarion Islands. The storm then moved into an environment of strong southerly shear later that evening as it approached a mid- to upper-level trough located to its northwest. Combined with increasingly cooler waters and a more stable air mass, the shear caused the low-level center to become separated from the deep convection early on

1 October, and Juliette weakened to a tropical depression later that day by 0000 UTC 2 October. No deep convection redeveloped, and Juliette degenerated to a remnant low at 1200 UTC 2 October. The forward motion of the remnant circulation slowed considerably, and the low became nearly stationary for about 24 h as it came under the influence of northwesterly flow associated with the low-level subtropical ridge. The low eventually began to move to the southeast, staying about 200 n mi west of the Baja California Peninsula, and ultimately degenerated to a trough at 0000 UTC 5 October.

*k. Tropical Storm Kiko, 15–23 October*

Kiko developed from a tropical wave that exited the coast of Africa on 26 September and initially spawned Tropical Storm Melissa over the eastern tropical Atlantic Ocean on 28 September. The southern portion of the wave continued westward and crossed into the eastern North Pacific basin around 8 October. A broad area of low pressure, accompanied by showers and thunderstorms, developed along the wave axis early on 11 October, while centered about 240 n mi south of Acapulco. As the system moved slowly west-northwestward, it remained disorganized for several days because of strong upper-level easterly winds. The upper-level winds abated somewhat, and the area of showers and thunderstorms associated with the low pressure improved in organization late on 13 October, while centered about 350 n mi south-southwest of Manzanillo. By 0000 UTC 15 October, the system had acquired sufficient organization to be classified as a tropical depression. The depression was initially embedded within a broad low-level cyclonic gyre with weak midtropospheric steering, and subsequently drifted southward for the next 30 h. Despite the moderate easterly shear, the tropical cyclone managed to produce a deep burst of convection early on 16 October close to the surface circulation center. The cyclone was briefly at tropical storm strength around 1200 UTC 16 October, while centered about 375 n mi southwest of Manzanillo.

This initial strengthening episode was short lived, however, and 6 h later visible satellite imagery depicted an exposed low-level circulation with convection located about 75 n mi southwest of the center, and Kiko weakened to a depression. The cyclone moved eastward to east-northeastward with a slowly increasing forward motion primarily due to the low-level steering.

Kiko became a tropical storm once again around 0600 UTC 17 October, while centered about 335 n mi south-southwest of Manzanillo. For the next couple of days, Kiko moved toward the east-northeast as a minimal tropical storm, toward the southwestern coast of Mexico within the low-level southwesterly flow on the south

side of the ITCZ. By 0000 UTC 19 October, Kiko turned toward the northwest as a ridge developed over Mexico. At this time, Kiko was located about 140 n mi south of Manzanillo and the associated convection was becoming better organized as a result of decreasing wind shear. During the next couple of days, Kiko slowly moved toward the northwest and gradually strengthened in response to light to moderate shear and warm waters.

Kiko reached its maximum intensity of 60 kt and minimum pressure of 991 mb at 1800 UTC 20 October, while centered about 150 n mi west-southwest of Manzanillo. Kiko maintained this intensity for about 12 h as it moved north-northwestward within a small break in the subtropical ridge. Thereafter, gradual weakening occurred due to both increasing southerly shear and a more stable environment. Kiko weakened to a tropical depression around 0000 UTC 23 October, while centered about 215 n mi west-southwest of Cabo Corrientes. Coming under the influence of a restrengthening deep-layer ridge to the north, the depression produced occasional bursts of deep convection while moving westward and west-southwestward until it degenerated into a remnant low around 0000 UTC 24 October. The remnant low continued to move generally westward for the next couple of days within the low-level steering flow. It then turned northward before dissipating on 27 October.

### 3. Forecast verification

For all operationally designated tropical (or subtropical) cyclones in the Atlantic and eastern North Pacific basins, the NHC issues an official forecast of the cyclone's center position and maximum 1-min surface wind speed. Forecasts are issued every 6 h and contain projections valid at 12, 24, 36, 48, 72, 96, and 120 h after the forecast's nominal initial time (0000, 0600, 1200, or 1800 UTC). At the end of the season, forecasts are evaluated by comparing the projected positions and intensities to the corresponding post storm derived "best track" positions and intensities of each cyclone. A forecast is included in the verification only if the system is classified in the best track as a tropical (or subtropical) cyclone at both forecast's initial time and the projection's valid time. All other stages of development (e.g., tropical wave, remnant low, and extratropical) are excluded. For verification purposes, forecasts associated with special advisories do not supersede the original forecast issued for that synoptic time; rather, the original forecast is retained. All verifications here include the depression stage.

It is important to distinguish between forecast error and forecast skill. Track forecast error is defined as the great-circle distance between a cyclone's forecast position and the best-track position at the forecast verification

TABLE 2. Homogenous comparison of official and CLIPER5 track forecast errors in the eastern North Pacific basin for the 2007 season for all tropical cyclones. Averages for the previous 5-yr period are shown for comparison.

	Forecast period (h)						
	12	24	36	48	72	96	120
2007 mean OFCL error (n mi)	30.0	50.2	71.4	92.5	117.2	146.9	186.3
2007 mean CLIPER5 error (n mi)	39.9	80.1	124.6	169.1	249.5	304.3	343.0
2007 mean OFCL error relative to CLIPER5 (%)	-24.8	-37.3	-42.7	-45.3	-53.0	-51.7	-45.7
2007 mean OFCL bias vector (°/n mi)	281°/7	279°/17	275°/30	269°/41	258°/44	231°/22	112°/37
2007 No. of cases	208	182	156	140	108	77	52
2002-06 mean OFCL error (n mi)	33.1	56.8	79.1	98.9	139.6	188.1	233.1
2002-06 mean CLIPER5 error (n mi)	39.4	76.8	117.8	155.1	225.2	286.7	351.4
2002-06 mean OFCL error relative to CLIPER5 (%)	-16.0	-26.0	-32.9	-36.2	-38.0	-34.4	-33.7
2002-06 mean OFCL bias vector (°/n mi)	319°/12	312°/3	310°/6	309°/12	301°/10	283°/6	270°/17
2002-06 No. of cases	1349	1192	1039	897	655	465	311
2007 OFCL error relative to 2002-06 mean (%)	-9.4	-11.6	-9.7	-6.5	-16.0	-21.9	-20.1
2007 CLIPER5 error relative to 2002-06 mean (%)	1.3	4.3	5.8	9.0	10.8	6.1	-2.4

time. Skill on the other hand, represents a normalization of forecast error against some standard or baseline. By convention, tropical cyclone forecast skill is positive when forecast errors are smaller than the errors from the baseline. Particularly useful skill standards are independent of operations (and hence can be applied retrospectively to historical data), and provide a measure of inherent forecast difficulty. For tropical cyclone track forecasts, the skill baseline is the Climatology and Persistence (CLIPER5) model, which contains no information about the current state of the atmosphere (Neumann 1972; Aberson 1998). The version of CLIPER5 presently in use is based on developmental data from 1931 to 2004 for the Atlantic and from 1949 to 2004 from the eastern Pacific.

Forecast intensity error is defined as the absolute value of the difference between the forecast and best-track intensity at the forecast verifying time. The skill of intensity forecasts is assessed using a modified version of the Statistical Hurricane Intensity Forecasts (SHIFOR5) climatology and persistent model (Jarvinen and Neumann 1979; Knaff et al. 2003). The modified model, known as DSHIFOR5, is constructed by taking the output from SHIFOR5 and applying the decay rate of DeMaria et al. (2006). The application of the decay component requires a forecast track, which here is given by CLIPER5. The use of DHIFOR5 as the intensity skill benchmark began in 2006. On average, DSHIFOR5 errors are about 5%–15% lower than SHIFOR5 in the Atlantic from 12 to 72 h, and about the same as SHIFOR5 at 96 and 120 h.

A comparison of the average track errors for 2007 to the previous 5-yr period for the official forecasts and the CLIPER5 model forecasts has been performed by

Franklin (2008) and is shown here in Table 2. The 2007 forecast track errors were lower than the previous 5-yr means at all forecast lead times, particularly for the 72-, 96-, and 120-h periods, when the errors were 16%, 22%, and 20% lower, respectively. These low errors occurred in a year when CLIPER errors were about 5%–10% above their long-term means, suggesting that the 2007 eastern North Pacific tropical cyclones were more difficult to forecast, on average. It is interesting to note that although the track errors were relatively small in 2007, forecast biases were much larger than average.

Table 3, also after Franklin (2008), is a verification of NHC official intensity forecasts to the Decay-SHIFOR5 model. The mean official intensity errors for 2007 were lower than the previous 5-yr mean for all periods except 96 h. However, as noted in Table 3, the average official intensity forecasts for 2007 were only skillful at the 12-, 24-, 36-, and the 120-h periods, when the mean forecast errors ranged from 3% to 14% lower than the corresponding SHIFOR5 errors for these forecast times. Decay-SHIFOR5 forecast errors in 2007 were lower than their 5-yr means, indicating that the season's storms were somewhat less difficult to forecast intensity than average. Eastern North Pacific intensity forecasts have traditionally had a high bias, and this was true again in 2007. A more detailed forecast verification for 2007 is given by Franklin (2008).

*Acknowledgments.* The cyclone summaries are based on tropical cyclone reports written by the authors and other NHC hurricane specialists: Jack Beven, Eric Blake, Daniel Brown, James Franklin, Richard Knabb, Michelle Mainelli, and Richard Pasch. Best-track data

TABLE 3. Homogenous comparison of official and Decay-SHIFOR5 intensity forecast errors in the eastern North Pacific basin for the 2007 season for all tropical cyclones. Averages for the previous 5-yr period are shown for comparison.

	Forecast period (h)						
	12	24	36	48	72	96	120
2007 mean OFCL error (kt)	5.1	8.2	11.6	14.4	18.1	20.8	17.0
2007 mean Decay-SHIFOR5 error (kt)	5.9	9.3	12.0	14.3	17.3	18.5	19.0
2007 mean OFCL error relative to Decay-SHIFOR5 (%)	-13.6	-11.8	-3.3	0.7	4.6	12.4	-10.5
2007 OFCL bias (kt)	1.2	2.3	3.9	4.4	3.8	1.3	-2.6
2007 No. of cases	208	182	156	140	108	77	52
2002-06 mean OFCL error (kt)	6.3	11.0	14.6	16.9	18.9	18.5	19.3
2002-06 mean Decay-SHIFOR5 error (kt)	7.2	12.0	15.7	18.4	21.5	21.5	21.1
2002-06 mean OFCL error relative to Decay-SHIFOR5 (%)	-12.5	-8.3	-7.0	-8.2	-12.1	-14.0	-8.5
2002-06 OFCL bias (kt)	0.7	1.9	2.8	2.6	4.1	3.9	1.4
2002-06 No. of cases	1349	1192	1039	896	655	465	311
2007 OFCL error relative to 2002-06 mean (%)	-19	-25	-20	-15	-4	12	-12
2007 Decay-SHIFOR5 error relative to 2002-06 mean (%)	-18	-22	-24	-22	-19	-14	-10

west of 140°W were provided by the Central Pacific Hurricane Center. Track charts and figures were produced with the help of Ethan Gibney and Joan David. Verification results and tables were provided by James Franklin. Local impacts for Mexico were provided mainly by the Mexican Weather Service.

#### REFERENCES

- Aberson, S. D., 1998: Five-day tropical cyclone track forecasts in the North Atlantic basin. *Wea. Forecasting*, **13**, 1005-1015.
- Avila, L. A., R. J. Pasch, J. L. Beven, J. L. Franklin, M. B. Lawrence, S. R. Stewart, and J. Jiing, 2003: Eastern North Pacific hurricane season of 2001. *Mon. Wea. Rev.*, **131**, 249-262.
- DeMaria, M., J. A. Knaff, and J. Kaplan, 2006: On the decay of tropical cyclone winds crossing narrow landmasses. *J. Appl. Meteor. Climatol.*, **45**, 491-499.
- Dvorak, V. F., 1984: Tropical cyclone intensity analysis using satellite data. NOAA Tech. Rep. NESDIS 11, National Oceanic and Atmospheric Administration, Washington, DC, 47 pp.
- Franklin, J. L., 2008: 2007 National Hurricane Center forecast verification report. NHC, 68 pp. [Available online at [http://www.nhc.noaa.gov/verification/pdfs/Verification\\_2007.pdf](http://www.nhc.noaa.gov/verification/pdfs/Verification_2007.pdf).]
- Jarvinen, B. R., and C. J. Neumann, 1979: Statistical forecasts of tropical cyclone intensity for the North Atlantic basin. NOAA Tech. Memo. NWS NHC-10, 22 pp.
- Knaff, J. A., M. DeMaria, C. R. Sampson, and J. M. Gross, 2003: Statistical, 5-day tropical cyclone intensity forecasts derived from climatology and persistence. *Wea. Forecasting*, **18**, 80-92.
- Neumann, C. B., 1972: An alternate to the HURRAN (hurricane analog) tropical cyclone forecast system. NOAA Tech. Memo. NWS SR-62, 24 pp.
- Pasch, R. J., and Coauthors, 2009: Eastern North Pacific hurricane season of 2006. *Mon. Wea. Rev.*, **137**, 3-20.
- Saffir, H. S., 1973: Hurricane wind and storm surge. *Mil. Eng.*, **423**, 4-5.
- Simpson, R. H., 1974: The hurricane disaster potential scale. *Weatherwise*, **27**, 169-186.

Copyright of *Monthly Weather Review* is the property of American Meteorological Society and its content may not be copied or emailed to multiple sites or posted to a listserv without the copyright holder's express written permission. However, users may print, download, or email articles for individual use.